한국소음진동공학회 2003년도 춘계학술대회논문집, pp. 47~56.

Free Vibration Analysis of Curved Beams in Cartesian Coordinates

직교좌표계에서 곡선보의 자유진동 해석

BYOUNG KOO LEE

Department of Civil and Environmental Engineering, Wonkwang University, Iksan, Junbuk 570-749, Korea

bkleest@wonkwang.ac.kr

이 병 구

원광대학교 토목환경도시공학부 토목환경공학전공

1. INTRODUCTION

Curved beams are one of the most important basic structural units as well as the beams, columns and plates. Most complicated structures consist of only these basic units and therefore it is very attractive research subject to analysis both the static and dynamic behavior of such units including the arches.

The problems of free vibrations of curved beams have been the subject of much work due to their many practical applications. Furthermore, characteristics of free vibrations of structures including arches are definitely unique, which are consequently used as an assessment index in evaluating the soundness of structures.

The governing equations and its significant historical literature on the free in-plane vibrations of elastic curved beams have been reported in many references for more than three decades. Background material for the current study was critically reviewed by Oh[1]. Briefly, such works included studies of the non-circular arches with predictions of only the lowest frequency in flexure by Romanelli and Laura[2], and in extension by Wang[3], and Wang and Moore[4]; studies of circular arches with predictions of the higher frequencies by Wolf[5] and Veletsos *et al.*[6]; studies of arches with variable curvature of the higher frequencies in flexure by Oh[1], Kang and Bert[7], Oh *et al.*[8], and Oh *et al.*[9]; and the effects of transverse shear and rotatory inertia on free vibration frequencies of arches by Irie *et al.*[10] and Davis *et al.*[11].

This paper has three main purposes: (1) to present the differential equations for free, planar vibrations of arches, i.e. vertically curved beam, with variable curvature and unsymmetric axis, where all equations are derived in Cartesian coordinates rather than in polar coordinates; (2) to include the effect of rotatory inertia in the differential equations; and (3) to illustrate the numerical solutions to the newly derived equations for a broad class of parabolic arches.

In most previous works on arch vibrations, the polar coordinates were employed and also the effect of unsymmetric axis was excluded in the parametric studies of vibration problems. The results presented herein extent significantly previous works. That is, using the Cartesian formulation together with highly efficient and convergent numerical methods, the free vibration frequencies and mode shapes, with and without the rotatory inertia, are investigated for parabolic arches with unsymmetric axis. Such numerical results are presented for both clamped ends and both hinged ends. The lowest four non-dimensional frequency parameters are shown as functions of three system parameters: the rise to chord length ratio, the span length to chord length ratio, and the slenderness ratio.

The following assumptions are inherent in this theory: the beam is linearly elastic; both tangential and radial displacements are considered; and the small deflection theory is governed. In addition, the beam is assumed to be in harmonic motion.

2. MATHEMATICAL MODEL

The geometry and nomenclature of the arch, i.e. vertically curved beam, placed in the Cartesian coordinates (x, y), with variable curvature and unsymmetric axis are shown in Fig. 1. The arch is supported by either both clamped ends or both hinged ends. The geometric variables are defined as follows.

L: Span length
l: Chord length
h: Rise
v: Tangential displacement
w: Radial displacement
ψ: Rotation of cross-section
ρ: Radius of curvature
θ: Inclination of ρ with x-axis

The shape of parabolic beam, which is chosen as the object arch with variable curvature herein, is expressed in terms of (l, h) and the coordinate x in the range from $x = 0$ to $x = L$. That is,

$$y = -(4h/l^2)x(x-l), \quad 0 \le x \le L \tag{1}$$

A small element of the beam is shown in Fig. 2 in which are defined the positive directions for the axial force N, the shear force Q, the bending moment M, the tangential inertia force F_v, the radial inertia force F_w, and the rotatory inertia couple C_ψ. Treating the inertia forces and the inertia couple as equivalent static quantities, the three equations for "dynamic equilibrium" of the element are

$$N' + Q + \rho F_v = 0 \tag{2}$$
$$Q' - N + \rho F_w = 0 \tag{3}$$
$$\rho^{-1}M' - Q - C_\psi = 0 \tag{4}$$

where $(')$ is the operator $d/d\theta$.

The equations that relate N, M and ψ to the displacements v and w[12] are

$$N = EA\rho^{-1}[(v' + w) + r^2\rho^{-2}(w'' + w)] \tag{5}$$
$$M = EAr^2\rho^{-2}(w'' + w) \tag{6}$$
$$\psi = \rho^{-1}(w' - v) \tag{7}$$

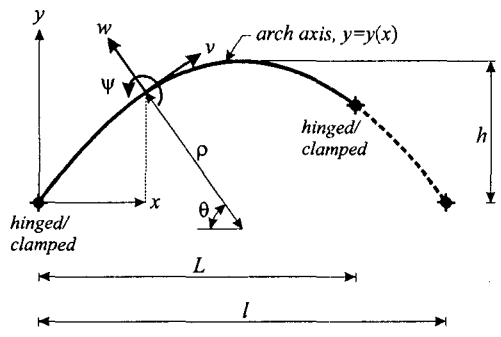

Fig. 1 Geometry of vertically curved beam and its variables

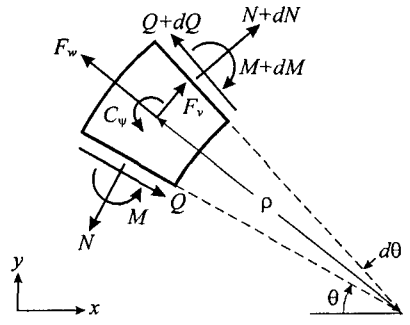

Fig. 2 Element subjected to stress resultants and inertia forces

where E is Young's modulus, A is the cross-sectional area and r is the radius of gyration of cross-section.

The arch is assumed to be in harmonic motion, or each coordinate is proportional to $\sin(\omega_i t)$ where ω_i is the i th circular frequency and t is time. Then the tangential and radial inertia forces, and rotatory inertia couple per unit arc length are, respectively,

$$F_v = m\omega_i^2 v \tag{8}$$

$$F_w = m\omega_i^2 w \tag{9}$$

$$C_\psi = m\omega_i^2 r^2 \psi = m\omega_i^2 r^2 \rho^{-1}(w' - v) \tag{10}$$

where m is the mass per unit arc length.

When Eqs. (5) and (6) are differentiated once, the results are

$$N' = EA\rho^{-1}[(v'' + w') + r^2\rho^{-2}\rho'(w''' + w') - \rho^{-1}\rho'(v' + w) - 3r^2\rho^{-3}\rho'(w'' + w)] \tag{11}$$

$$M' = -EAr^2\rho^{-2}[(w''' + w') - 2\rho^{-1}\rho'(w'' + w)] \tag{12}$$

When Eqs. (10) and (12) are substituted into Eq. (4), then

$$Q = \rho^{-1}M' - RC_\psi = -EAr^2\rho^{-3}[(w''' + w') - 2\rho^{-1}\rho'(w'' + w)] - Rm\omega_i^2 r^2\rho^{-1}(w' - v) \tag{13}$$

where the index R is defined as follows.

$R = 1$ if rotatory inertia C_ψ is included. (14.1)

$R = 0$ if rotatory inertia is excluded. (14.2)

The following equation is obtained by differentiating Eq. (13).

$$\begin{aligned} Q' = &-EAr^2\rho^{-3}[(w'''' + w'') - 5\rho^{-1}\rho'(w''' + w') + 2\rho^{-1}(4\rho^{-1}\rho'^2 - \rho'')(w'' + w)] \\ &- Rm\omega_i^2 r^2\rho^{-1}[(w'' - v') - \rho^{-1}\rho'(w' - v)] \end{aligned} \tag{15}$$

From Fig. 1, it is seen that the inclination θ is related to the coordinate x. By the mathematical definition,

$$\theta = \pi/2 - \tan^{-1}(dy/dx) = \pi/2 - \tan^{-1}[-(4hl^{-2})(2x - l)] \tag{16}$$

When Eq. (16) is differentiated, the result is

$$d\theta = (8hl^2)/[l^4 + 16h^2(2x - l)^2]dx \tag{17}$$

Define the following arch parameters.

$$g_1 = [l^4 + 16h^2(2x - l)^2]/(8hl^2) \tag{18.1}$$

$$g_2 = 8h(2x - l)/l^2 \tag{18.2}$$

$$g_3 = 16h/l^2 \tag{18.3}$$

From Eq. (17), and with Eqs. (18.1)-(18.3), the following differential operators are obtained.

$$\frac{d}{d\theta} = g_1 \frac{d}{dx} \tag{19}$$

$$\frac{d^2}{d\theta^2} = g_1^{\,2} \frac{d^2}{dx^2} + g_1 g_2 \frac{d}{dx} \tag{20}$$

$$\frac{d^3}{d\theta^3} = g_1^{\,3} \frac{d^3}{dx^3} + 3g_1^{\,2} g_2 \frac{d^2}{dx^2} + g_1(g_1 g_3 + g_2^{\,2}) \frac{d}{dx} \tag{21}$$

$$\frac{d^4}{d\theta^4} = g_1^{\,4} \frac{d^4}{dx^4} + 6g_1^{\,3} g_2 \frac{d^3}{dx^3} + g_1^{\,2}(4g_1 g_3 + 7g_2^{\,2}) \frac{d^2}{dx^2} + g_1 g_2(4g_1 g_3 + g_2^{\,2}) \frac{d}{dx} \tag{22}$$

The radius of curvature ρ at any point of the parabolic arch is expressed as Eq. (23). Also, its derivatives ρ' and ρ'' can be expressed in terms of x by using Eq. (23) with Eqs. (19) and (20) as Eqs. (24) and (25), respectively. That is,

$$\rho = [1 + (dy/dx)^2]^{3/2} (d^2 y/dx^2)^{-1} = (1/\sqrt{2}) g_1^{\,3/2} g_3^{\,1/2} \tag{23}$$

$$\rho' = (3\sqrt{2}/4) g_1^{\,3/2} g_2 g_3^{\,1/2} \tag{24}$$

$$\rho'' = (3\sqrt{2}/8) g_1^{\,3/2} g_3^{\,1/2} (2g_1 g_3 + 3g_2^{\,2}) \tag{25}$$

Now cast the differential equations of free vibration for the arch into non-dimensional form by introducing the non-dimensional parameters as follows.

$$\xi = x/l \tag{26}$$

$$\eta = y/l \tag{27}$$

$$f = h/l \tag{28}$$

$$e = L/l \tag{29}$$

$$\lambda = v/l \tag{30}$$

$$\delta = w/l \tag{31}$$

$$s = l/r \tag{32}$$

Here the coordinates (x, y), the rise h, the span length L, and the displacements v and w are normalized by the chord length l, and s is the slenderness ratio.

When Eqs. (5), (9), and (15) together with Eqs. (18)-(32) are used in Eq. (3), the result is Eq. (33). Also, when Eqs. (8), (11) and (13) are combined with Eqs. (2), the result is Eq. (34). That is,

$$\delta^{iv} = a_1 \delta^{iii} + (a_2 + Rc_i^{\,2} a_3)\delta^{ii} + (a_4 + Rc_i^{\,2} a_5)\delta^{i} + (a_6 + c_i^{\,2} a_7)\delta + c_i^{\,2}(a_8 + Ra_9)\lambda^{i} + Rc_i^{\,2} a_{10}\lambda \tag{33}$$

$$\lambda^{ii} = a_{11}\delta^{ii} + (a_{12} + Rc_i^{\,2} a_{13})\delta^{i} + a_{14}\delta + a_{15}\lambda^{i} + c_i^{\,2}(a_{16} + Ra_{17})\lambda \tag{34}$$

where $(^{i})$ is the operator $d/d\xi$, and the constants of a_1 through a_{17} are as follows.

$$a_1 = 1.5 b_1^{-1} b_2 \tag{35.1}$$

$$a_2 = -b_1^{-2}(64 f b_1 + 2.5 b_2^{\,2} - b_3 + 2) \tag{35.2}$$

$$a_3 = -8 f s^{-2} b_1 \tag{35.3}$$

$$a_4 = b_1^{-3} b_2 (56 f b_1 - 11.5 b_2^{\,2} + b_3 + 5.5) \tag{35.4}$$

$$a_5 = 4 f s^{-2} b_2 \tag{35.5}$$

$$a_6 = -b_1^{-4}(8 f s^2 b_1^{\,3} + 18 b_2^{\,2} - b_3) \tag{35.6}$$

$$a_7 = 64 f^2 b_1^{\,2} \tag{35.7}$$

$$a_8 = -8fs^2 \tag{35.8}$$

$$a_9 = 8fs^{-2} \tag{35.9}$$

$$a_{10} = -12fs^{-2}b_1^{-2}b_2 \tag{35.10}$$

$$a_{11} = 0.1875f^{-1}s^{-2}b_1^{-3}b_2 \tag{35.11}$$

$$a_{12} = 0.1875f^{-1}s^{-2}b_1^{-4}b_2^{2} - b_1^{-1} \tag{35.12}$$

$$a_{13} = s^{-4}b_1^{-1} \tag{35.13}$$

$$a_{14} = 1.5b_1^{-2}b_2(0.125f^{-1}s^{-2}b_1^{-3} + 1) \tag{35.14}$$

$$a_{15} = 0.5b_1^{-1}b_2 \tag{35.15}$$

$$a_{16} = -8fs^{-2}b_1 \tag{35.16}$$

$$a_{17} = -s^{-4}b_1^{-2} \tag{35.17}$$

where,

$$b_1 = 0.125f^{-1}[1 + 16f^2(2\xi - 1)^2] \tag{36.1}$$

$$b_2 = 8f(2\xi - 1) \tag{36.2}$$

$$b_3 = 6[1 + 64f^2(2\xi - 1)^2] \tag{36.3}$$

In Eqs. (33) and (34), The non-dimensional frequency parameter is defined as

$$c_i = \omega_i r^{-1} l^2 \sqrt{m/(EA)} = \omega_i l^2 \sqrt{\gamma A/(EI)}, \quad i = 1, 2, 3, 4, \Lambda \tag{37}$$

where γ is the mass density.

Now consider the boundary conditions. At a clamped end ($x = 0$ or $x = L$), the boundary conditions are $v = w = \psi = 0$ and these relations can be expressed in the non-dimensional form as

$$\lambda = 0 \text{ at } \xi = 0 \text{ or } \xi = e \tag{38}$$

$$\delta = 0 \text{ at } \xi = 0 \text{ or } \xi = e \tag{39}$$

$$\delta^i = 0 \text{ at } \xi = 0 \text{ or } \xi = e \tag{40}$$

Here, the latest Eq. (40) implies that the rotation of cross-section ψ expressed in Eq. (7) is zero.

At a hinged end ($x = 0$ or $x = L$), the boundary conditions are $v = w = M = 0$ and these relations can be expressed in the non-dimensional form as

$$\lambda = 0 \text{ at } \xi = 0 \text{ or } \xi = e \tag{41}$$

$$\delta = 0 \text{ at } \xi = 0 \text{ or } \xi = e \tag{42}$$

$$\delta^{ii} + b_1^{-1}b_2\delta^i = 0 \text{ at } \xi = 0 \text{ or } \xi = e \tag{43}$$

Also, the latest Eq. (43) implies that the bending moment M expressed in Eq. (6) is zero.

3. NUMERICAL METHODS AND DISCUSSION

Based on the above analysis, a general FORTRAN computer program was written to calculate the frequency parameters c_i and the corresponding mode shapes $\lambda = \lambda_i(\xi)$, $\delta = \delta_i(\xi)$ and $\psi = \psi_i(\xi)$. The numerical methods described by Oh[1], and Lee *et al.*[13] were used to solve the differential Eqs. (33) and (34),

subjected to the end constraint Eqs. (38)-(40) or Eqs. (41)-(43). First, the Determinant Search method combined with the Regula-Falsi method[14] was used to obtain the frequency parameter c_i, and then the Runge-Kutta method[14] was used to calculate the mode shapes λ, δ and ψ.

Prior to executing the numerical studies, the convergence analysis, for which $f = 0.3$, $e = 0.8$, $s = 50$, and $R = 1$, was conducted to determine the appropriate step size $\Delta\xi$ in the Runge-Kutta method. Figure 3 shows $1/\Delta\xi$ versus c_i curves, in which a step size of $1/\Delta\xi = 20$ is found to give convergence for c_i to within three significant figures. It is noted that the convergence efficiency herein is highly promoted, under same convergence criteria, comparing the appropriate $1/\Delta\xi = 50$ obtained by Oh[1] in polar coordinates. However, the step size of $\Delta\xi = 1/50$ was used herein in order to increase accuracy of numerical solutions.

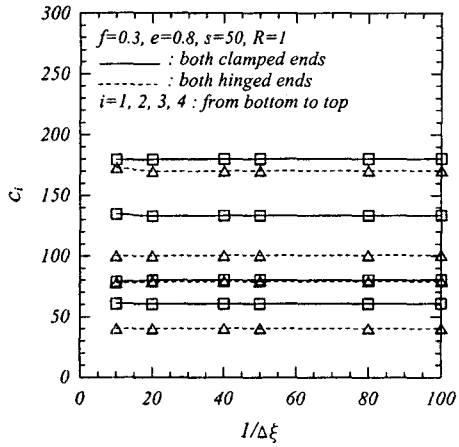

Fig. 3 Convergence analysis

Four lowest values of $c_i (i = 1,2,3,4)$ and the corresponding mode shapes were calculated in this study. Numerical results, given in Table 1, Table 2 and Figs. 4 through 7, are now discussed. The first series of numerical results are shown in Table 1. These studies served as an approximate check on the analysis presented herein. For comparative purposes, finite element solutions based on the commercial packages SAP 2000 were used to compute the first four frequency parameters c_i for both clamped ends and both hinged ends. The results showed that the 100 finite elements were necessary to match within a tolerance of about 2.5% values of c_i computed by solving the governing differential equations.

Table 1 Comparisons of c_i between this study and SAP 2000

Geometry	i	Frequency parameter, c_i		Ratio*
		This study	SAP 2000	
Both clamped ends, $f = 0.3, e = 0.8,$ $s = 50, R = 1$	1	60.13	60.30	0.997
	2	80.12	80.96	0.990
	3	133.5	136.9	0.975
	4	180.4	181.2	0.996
Both hinged ends, $f = 0.3, e = 0.8,$ $s = 50, R = 1$	1	40.34	40.92	0.986
	2	79.07	80.42	0.983
	3	100.6	100.9	0.997
	4	170.5	173.6	0.982

* Ratio=(This study)/(SAP 2000)

All of numerical results that follow are based on the analysis reported herein. The effects of rotatory inertia on natural frequencies are shown in Table 2. It is apparent that the effect of rotatory inertia is to always depress the natural frequencies, in which these depressions are less than about 3 %. Further, the frequencies of both clamped ends are always greater than those of both hinged ends, other parameters remaining the same.

Table 2 Effect of rotatory inertia on frequency parameter

Geometry	i	Frequency parameter, c_i		Ratio*
		$R=0$	$R=1$	
Both clamped ends, $f=0.3, e=0.8,$ $s=50$	1	61.05	60.13	0.985
	2	80.44	80.12	0.996
	3	136.0	133.5	0.982
	4	181.4	180.4	0.994
Both hinged ends, $f=0.3, e=0.8,$ $s=50$	1	40.59	40.34	0.993
	2	79.35	79.07	0.996
	3	102.7	100.6	0.980
	4	174.5	170.5	0.977

* Ratio $=(R=1)/(R=0)$

It is shown in Fig. 4, for which $e=0.8$, $s=50$ and $R=1$, that each frequency curve of second modes of both clamped ends and both hinged ends reaches a peak as the horizontal rise to chord length ratio f is increased while the other frequency parameters decrease as f is increased. Further, it is observed for these unsymmetric arch configurations that two mode shapes can exist at a single frequency, a phenomena that was previously observed only for symmetric arch configurations[1]. For both hinged ends, the first and second modes have the same frequency $c_1=c_2=53.06$ at $f=0.153$ (marked as ■). However, the frequency curves of first and second modes for both clamped ends come close each other but not cross.

It is shown in Fig. 5, for which $f=0.3$, $s=50$ and $R=1$, that the frequency parameters c_i decrease as the span length to chord length ratio e is increased. Particularly, it is noted that the frequency parameters of third and fourth modes are more significantly decreased as e gets smaller value.

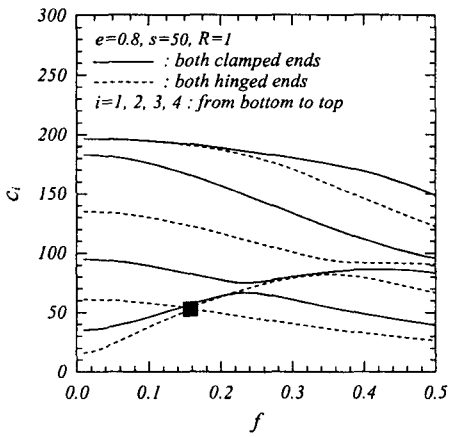

Fig. 4 c_i versus f curves

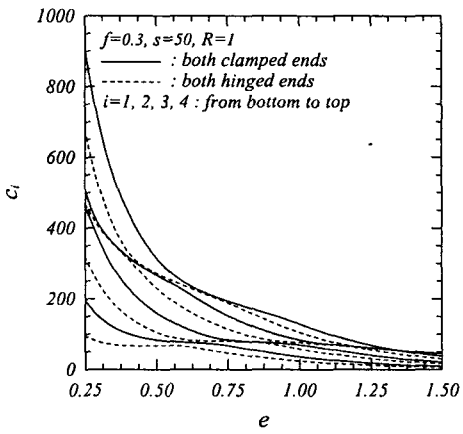

Fig. 5 c_i versus e curves

It is shown in Fig. 6, for which $f=0.3$, $e=0.8$ and $R=1$, that the frequency parameters c_i increase, and in most cases approach a horizontal asymptote, as the slenderness ratio s is increased. Further, it is seen from Tables 1 and 2, and Figs. 3 through 6 mentioned above that the frequencies of both clamped ends are always greater than those of both hinged ends, other parameters remaining the same.

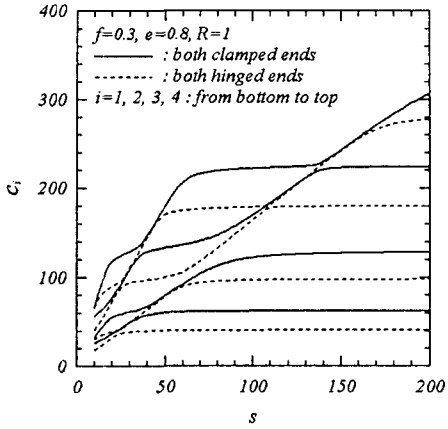

Fig. 6 c_i versus s curves

Figure 7 shows the computed mode shapes with $f=0.3$, $e=0.8$, $s=50$ and $R=1$ for both clamped ends and both hinged ends. From these figures, the amplitude and the positions of maximum amplitude and nodal points of each mode can be obtained, which is widely used in the fields of vibration control.

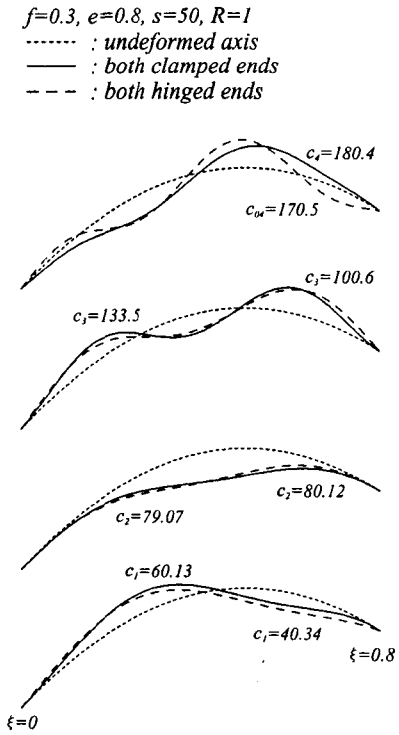

Fig. 7 Example of mode shapes

4. CONCLUDING REMARKS

This study deals with the free vibrations of curved beams with unsymmetric axis. The governing differential equations are derived in Cartesian coordinates rather than in polar coordinates, in which the effect of rotatory inertia on the natural frequency is included. The differential equations, subjected to parabolic curved beams, newly derived herein were solved numerically to calculate both natural frequencies and mode shapes. For validating the theories and numerical methods presented herein, frequency parameters obtained in this study are compared to those of SAP 2000. The convergent efficiency of numerical methods developed herein is highly improved under the differential equations in Cartesian coordinates. As the numerical results, the relationships between the frequency parameters and the various non-dimensional arch parameters are reported, and typical mode shapes are presented. It is expected that results obtained herein can be practically utilized in the fields of vibration control.

REFERENCES

1. Oh, S.J., 1996, Free vibrations of arches with variable cross-section, Ph.D. Dissertation, Wonkwang University, Iksan, Korea.
2. Romanelli, E. and Laura, P.A.A., 1972, "Fundamental frequency of non-circular, elastic, hinged arcs," *Journal of Sound and Vibration*, 24(1), pp. 17-22.
3. Wang, T.M., 1972, "Lowest natural frequency of clamped parabolic arcs," *Journal of the Structural Division,* ASCE, 98(ST1), pp. 407-411.
4. Wang, T.M. and Moore, J.A., 1973, "Lowest natural extensional frequency of clamped elliptic arcs," *Journal of Sound and Vibration*, 30(1), pp. 1-7.
5. Wolf, Jr. J.A., 1971, "Natural frequencies of circular arches," *Journal of the Structural Division,* ASCE, 97(ST9), pp. 2337-2350.
6. Veletsos, A.S., Austin, A.J., Pereira, C.A.L. and Wung, S.J., 1972, "Free in-plane vibrations of circular arches," *Journal of Engineering Mechanics Division, ASCE*, 93, pp. 311-329.
7. Kang, KJ. and Bert, C.W., 1995, "Vibration analyses of shear deformable circular arches by the differential quadrature method," *Journal of Sound and Vibration*, 181, pp. 353-360.
8. Oh, S.J., Lee, B.K. and Lee, I.W., 1999, "Natural frequencies of non-circular arches with rotatory inertia and shear deformation," *Journal of Sound and Vibration*, 219(1), pp. 23-33.
9. Oh, S.J., Lee, B.K. and Lee, I.W., 2000, "Free vibrations of non-circular arches with non-uniform cross-section," *International Journal of Solids and Structures,* 37(36), pp. 4871-4891.
10. Irie, T. and Yamada G. and Tanaka, K., 1983, "Natural frequencies of in-plane vibration of arcs," *Journal of Applied Mechanics,* ASME, 50, pp. 449-4527.
11. Davis, R., Henshell, R.D. and Warburton, G.B., 1972, "Constant curvature beam finite elements for in-plane vibration," *Journal of Sound and Vibration*, 25(4), pp. 561-576.
12. Borg and Gennaro, 1957, *Advanced Structural Analysis,* McGrow-Hill Book Company.
13. Lee, B.K., Oh, S.J. and Park. K.K., 2002, "Free vibrations of shear deformable circular curved beams resting on an elastic foundation," *International Journal of Structural Stability and Dynamics*, 2(1), pp. 77-97.
14. Al-Khafaji, A.W. and Tooley, J.R., 1986, *Numerical Method in Engineering Practice*, Holt, Reinhardt and Winston, Inc.